

# Relativistic collapse of axion stars

Florent Michel<sup>1,\*</sup> and Ian G. Moss<sup>2,†</sup>

<sup>1</sup>*Centre for Particle Theory, Durham University, South Road, Durham, DH1 3LE, UK*

<sup>2</sup>*School of Mathematics, Statistics and Physics, Newcastle University, Newcastle Upon Tyne, NE1 7RU, UK*

(Dated: July 30, 2018)

We study the gravitational collapse of an axion field in null coordinates, assuming spherical symmetry. Compared with previous studies, we use a simpler numerical scheme which can run, for relevant parameters, in a few minutes or less on a desktop computer. We use it to accurately determine the domains of parameter space in which the axion field forms a black hole, an axion star or a relativistic Bosenova.

## I. INTRODUCTION

Amongst the possible dark matter candidates, a coherent scalar field with very low mass is an enticing possibility. The idea originated with the QCD axion [1], but the concept has since been extended to a class of axion-like particles (ALP's) with ultra-light masses [2]. In ALP scenarios, the dark matter forms gravitationally bound objects which may form into galaxy cores [3], or for larger masses into axion mini-clusters [4–6]. These objects are often stable only for a particular mass range, leaving the possibility of detectable cosmological signatures from the axion bound structures or from the remnants of their collapse.

ALP's are characterised by their mass  $m$  and decay constant (or symmetry breaking scale)  $f$ . Coherent ALP dark matter scenarios envision the dark matter energy density in the form of large-scale coherent axion oscillations of frequency  $\sim m$ , with density parameter [1]

$$\Omega_{\text{ALP}} \sim 0.1 \left( \frac{f}{10^{17} \text{ GeV}} \right)^2 \left( \frac{m}{10^{-22} \text{ eV}} \right)^{1/2}, \quad (1)$$

although this is rather dependent on initial conditions. Spatial gradients in the oscillating axion field induce “quantum” pressure forces which are capable of supporting structures on the Kpc scale for axion masses around  $m \sim 10^{-22}$  eV, or galaxy Halo scales for  $m \sim 10^{-24}$  eV [2].

We follow the recent trend of referring to stable axion structures as axion stars (though the term Bose star is also frequently used in this context). So far three distinct scenarios of gravitational collapse for APL's have been identified [7, 8]: they can settle down quietly to an axion star; they can radiate away energy in bursts of relativistic axions or they can collapse to a black hole. The second outcome is a relativistic analogue of the Bosenova phenomena in cold-atom physics [9]. Like the cold atoms in a Bosenova, the axions have an attractive self-interaction force which can overcome the quantum pressure. We will use the term Bosenova in this paper to refer to the axion collapse and radiation phenomenon.

The fate of an axion clump can be represented on phase diagrams labelled by parameters describing the axion properties and the initial conditions. Recently, Helfer et al. [8] have produced a phase diagram for spherically symmetric collapse with axion decay constant  $f$  and the initial mass of the axion clump, and they have speculated that there is a tricritical point joining phase boundaries between the three outcomes. The aim of this paper is to provide convincing numerical evidence for the tricritical point using a particularly amenable form of the field equations, and to determine the parameter values accurately at the phase boundaries.

We use the null-coordinate integration schemes introduced into spherically symmetric gravitational collapse by Goldwirth and Piran [10]. The null techniques are particularly efficient because the coordinate grid flows inwards with the collapsing matter. For example, the null methods can reproduce the universal scaling phenomena in massless scalar collapse [11], which otherwise is only possible with less efficient mesh refinement techniques [12].

Throughout this work, we use units in which the reduced Planck constant  $\hbar$  and velocity of light  $c$  are equal to unity. The reduced Planck mass  $M_p = (8\pi G)^{-1/2}$ , where  $G$  is Newton's constant.

---

\* florent.c.michel@durham.ac.uk

† ian.moss@newcastle.ac.uk

## II. MODEL AND FIELD EQUATIONS

We take the generic axion potential  $V$ , which is typical of the potentials which represent axion dark matter [13–15]:

$$V(\phi) = m^2 f^2 \left( 1 - \cos\left(\frac{\phi}{f}\right) \right). \quad (2)$$

The parameters  $m$  and  $f$  are related by (1) if the cosmological dark matter density is in the form of coherent axion oscillations, but we will generally take  $m$  and  $f$  as free parameters. The Lagrangian density of the axion field is

$$\mathcal{L}_\phi = -\frac{g^{\mu\nu}}{2} (\partial_\mu \phi) (\partial_\nu \phi) - V(\phi), \quad (3)$$

where  $g_{\mu\nu}$  is the metric.

The focus of this paper is on spherically-symmetric collapse. Following [10, 11, 16], we use a very efficient integration scheme obtained by introducing the retarded time coordinate  $u$  and radial coordinate  $r$ , with metric

$$ds^2 = -g(u, r) \bar{g}(u, r) du^2 - 2g(u, r) du dr + r^2 d\Omega^2. \quad (4)$$

As usual,  $d\Omega^2$  is the metric on the unit sphere, and we suppose that  $g, \bar{g}$  are two smooth functions. Without loss of generality, up to a redefinition of  $u$ , we can impose boundary conditions at the origin,  $\bar{g}(u, 0) = 1$ . Imposing that there is no conical singularity at  $r = 0$  then implies that  $g(u, 0) = 1$  [10].

We follow the conventions of [10, 11] and introduce the notation  $\bar{h}$  for the scalar field  $\phi$ . Radial derivatives of  $\bar{h}$  are used to define an auxiliary field  $h$ . One can show that the Einstein equations are fully equivalent to a system of first order equations:

$$\partial_u h - \frac{\bar{g}}{2} \partial_r h = \frac{h - \bar{h}}{2r} \left[ (1 - 8\pi G r^2 V(\bar{h})) g - \bar{g} \right] - \frac{g}{2} r V'(\bar{h}), \quad (5)$$

$$\partial_r \ln(g) = \frac{4\pi G}{r} (h - \bar{h})^2, \quad (6)$$

$$\partial_r (r \bar{g}) = (1 - 8\pi G r^2 V(\bar{h})) g, \quad (7)$$

$$\partial_r (r \bar{h}) = h, \quad (8)$$

The first of these equations is a form of the Klein-Gordon equation which can be integrated using the method of characteristics. Starting from the initial data surface  $u = 0$ , we label the ingoing radial null geodesics by a coordinate  $v$ . The ingoing null geodesics for the metric Eq. (5) satisfy the characteristic equation for (5),

$$\partial_u r|_v = -\frac{\bar{g}}{2}. \quad (9)$$

Changing to null coordinates, so that  $h(u, r)$  becomes  $h(u, v)$ , gives the evolution along the characteristic surfaces of constant  $v$ ,

$$\partial_u h = \frac{h - \bar{h}}{2r} \left[ (1 - 8\pi G r^2 V(\bar{h})) g - \bar{g} \right] - \frac{g}{2} r V'(\bar{h}), \quad (10)$$

In order to solve these field equations, we have adapted the numerical procedure from Refs. [10, 11, 17]. Starting from given initial data for  $\bar{h}$  and  $r$  at  $u = 0$ , we first compute  $h(0, v)$ ,  $g(0, v)$ , and  $\bar{g}(0, v)$  using (6–8). We evolve  $r$  and  $h$  in the  $u$  direction using Equations (9) and (10), discarding points for which  $r$  becomes negative. At each step, the constraints (6–8) are solved by integrating in the  $v$  direction.

Evolution methods based on the 3+1 space and time coordinates solve their constraints on the initial time hypersurface, usually as a boundary value problem, and can be subject to constraint violation at later times. This is not an issue with the null coordinate formalism. The method only requires us to solve the *ordinary* differential equations, (10) and (9), with integrations over  $v$  at each time step. As a result, the method is remarkably accurate, fast and reliable.

When a black hole forms, it is possible to follow the evolution up to the null surface  $u = u_T$  which contains a marginally trapped surface at  $r = r_T$ . We define the final black hole mass  $M_H$  as the Bondi mass [18, 19],

$$M_H = \lim_{u \rightarrow u_T} \lim_{v \rightarrow \infty} \frac{r}{2G} \left( 1 - \frac{\bar{g}}{g} \right), \quad (11)$$

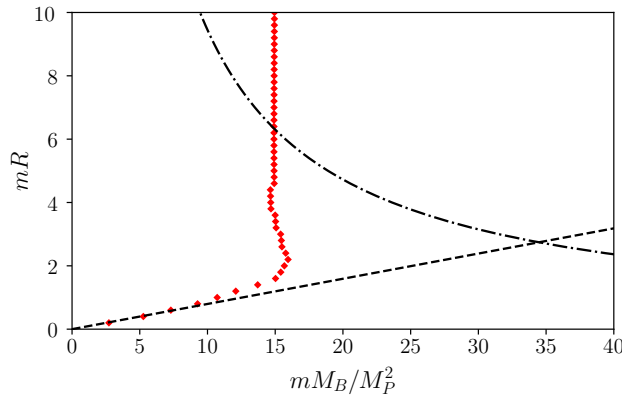


Figure 1. This plot shows the phase plane for the collapse of a massive scalar field without self-interaction, for an initial profile of the form (13). The two parameters used are the initial Bondi mass  $M_B$  and the initial radius  $R$ , scaled with the axion mass  $m$ . The dots show the boundary between black hole formation (left) and boson stars (right). The dashed line shows  $R = 2GM_B$ , i.e., the mass of a static black hole of radius  $R$ . The dash-dot line shows the mass-radius relation for a non-relativistic boson star.

since this is appropriate for null coordinate systems. A Schwarzschild black hole metric with mass  $M$ , for example, has  $g = 1$ ,  $\bar{g} = 1 - 2GM/r$  and  $M_H = M$ . At the marginally trapped surface  $g \rightarrow \infty$ , and the computational grid has to be compressed to counter the growth in the right hand side of (10). In practice, the integration is stopped when  $\bar{g}/g$  reaches a predetermined value. The Bondi mass is calculated at the final value of  $u$  and with  $v$  at the extreme edge of the coordinate grid.

Removing the limits from (11) gives a local quantity  $M_B(u, v)$  which evolves according to

$$\partial_u M_B = -2\pi r^2 \left( \frac{2}{g} (\partial_u \bar{h})^2 + \bar{g} V(\bar{h}) \right). \quad (12)$$

When  $g$ ,  $\bar{g}$ , and  $V$  are positive, then  $\partial_u M_B \leq 0$ . We will use  $-\partial_u M_B$  as a measure of the energy flux from the collapsing star. Any increase of  $M$  along in the ingoing null direction indicates (at least if  $V$  remains positive) an artefact from the numerical integration, and the corresponding runs are discarded. We can also use (12) to put bounds on the error in the black hole mass from truncating the integration before the trapped surface at  $u = u_T$ . This gives better control of the black hole mass than we would have using the mass at the trapped surface,  $r_T/2G$ , which was used in previous work.

### III. NUMERICAL RESULTS

We preface the full analysis with some results on the collapse of a massive, real, scalar field without self-interaction. Depending on initial conditions, the system can collapse to a black hole or a stable oscillaton, i.e. an oscillating field configuration that maintains its radial profile [5, 6]. The phase diagram for relativistic collapse in terms of mass and radius was obtained semi-analytically in Ref. [20]. The fully relativistic collapse of a massive scalar field was studied in some detail using null coordinates in Ref. [16] and using a 3+1 approach in Ref. [21].

We use the null coordinate approach to plot the phase diagram in terms of the axion mass  $m$ , the initial radius  $R$  and Bondi mass  $M_B$ . The choice of initial density profile is somewhat arbitrary, but we choose to work with a Gaussian profile which has been used previously for Bose stars [22]. The scalar field is oscillatory in time, and when projected on to the light-cone in flat space,

$$\bar{h}_i(r) = \sqrt{\frac{2M}{\pi^{3/2} m^2 R^3}} e^{-r^2/(2R^2)} \cos(mr). \quad (13)$$

The pre-factor has been chosen so that the mass of the star is  $M$  in the non-relativistic limit  $Rm \gg 1$ . The relationship between the radius and the ingoing null coordinate on the initial surface can be specified freely, but the uniform choice  $r = 2v$  will be used for simplicity. Initial conditions on the remaining fields are determined by the constraints (6-8), which ensure that we have a consistent set of initial conditions for the fully relativistic collapse.

The metric and scalar fields are evolved using the method described above. After dimensional rescaling, the solutions only depend on the initial parameters in the combinations  $mR$  and  $mM_B/M_P^2$ . Figure 1 shows the phase diagram

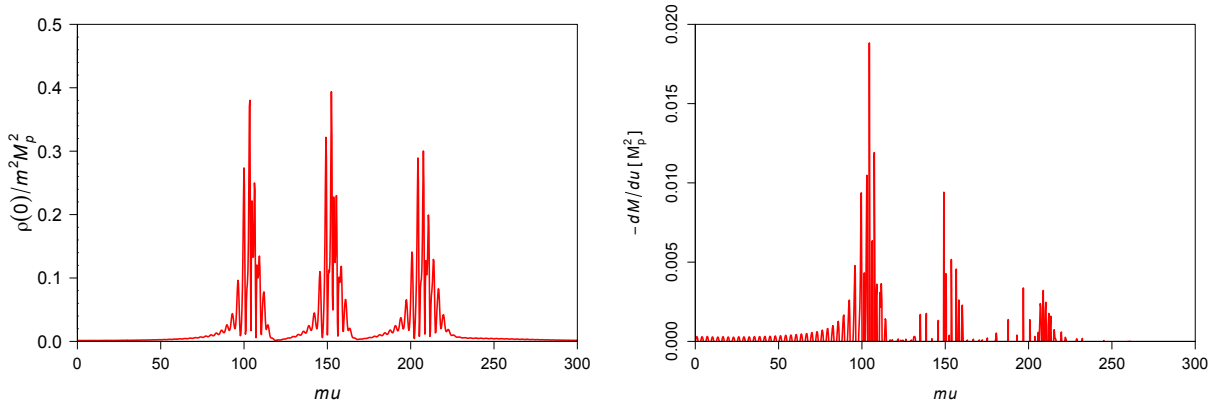


Figure 2. The central density (left) and the energy flux (right) for a collapsing Bosenova are plotted against the retarded time  $u$ . The flux is measured on the outer null edge of the integration volume,  $mv = 10^3$ . In this example  $mM_B/M_p^2 = 8.9$ , where  $m$  is the axion mass,  $M_B$  is the Bondi mass, and the axion scale  $f = 0.1M_p$ . The plot shows density spikes inside the star which produce pulses of axion radiation travelling at close to the speed of light.

for collapse in terms of these rescaled parameters. When the mass and radius are appropriate for a stable axion star, the scalar field profile settles down to the axion star field profile within a few oscillations. The phase transition boundary is traced out by dots, obtained by a bisection search technique. The condition for black hole collapse becomes nearly independent of radius when  $mR \gtrsim 2$ , with critical Bondi mass  $M_B \approx 15.22M_p^2m^{-1}$  and mass parameter  $M \approx 15.55M_p^2m^{-1}$ . The Bondi mass is in very good agreement with the results of the 3+1 approach, where the critical ADM mass is  $M_{ADM} \approx 15.2M_p^2m^{-1}$  (after accounting for the switch from Planck mass to reduced Planck mass) [21].

Inclusion of self-interaction leads to a third possible outcome of gravitational collapse, a Bosenova, where the collapsing field loses mass in pulses of axion radiation. The possibility of collapse due to self-interaction was first noticed in the non-relativistic limit [22, 23], but the radiation is highly relativistic, as pointed out in Ref. [7]. A fully relativistic treatment of axion collapse with general relativity was given in Ref. [8]. The phase plane of mass and axion scale was also discussed in [8], where evidence was given for the existence of a tri-critical point between the three outcomes. We make use of our rapid integration scheme to give a clearer picture of the phase plane.

The Gaussian profile is used for the initial data as before, but with fixed initial radius. It is desirable to have stable axion stars settle down as quickly as possible to their final form in order to keep down the integration time. In order to achieve this, we choose the initial radius using the radius for non-relativistic Bose stars [22, 23],  $R \approx 2(24\pi^3)^{1/2}M_p^2/Mm^2$ . Figure 1 shows that this radius lies in the region of the phase diagram where the dependence on radius is weak.

The Bosenova is characterised by collapses of the stellar core followed by bursts of axion radiation. The collapse and burst pattern is repeated until a significant portion of the initial mass has been radiated away. An example is illustrated in figure 2, which shows the central density and the radiation escaping at the edge of the integration volume as functions of retarded time. The radiation escapes a short retarded time after each collapse, indicating that the radiation is highly relativistic. Burst can be highly irregular, both in their timing and amplitude. When a black hole forms instead of a Bosenova, this tends to happen at the same retarded time as the first spike in the central density.

The phase diagram is shown in figure 3. There is a tricritical point in agreement with Ref. [8], but the mass and axion scale at the tricritical point are substantially different from the earlier results. The difference is too large to be explained by the difference between using initial conditions on a null surface instead of a timelike surface. Our results are broadly consistent with the non-relativistic limit though, where there is a critical mass for the collapse of a Bose star [22, 23],  $M \approx 50.77fM_p/m$ , shown on figure 3.

The phase boundary between axion stars and black holes is sharply defined, and the mass of the black hole is discontinuous at the phase boundary. However, the phase boundary between black holes and Bosenovas becomes diffuse at small values of the axion scale parameter  $f$ , in the sense that there is a range of masses near the phase boundary where the outcome of gravitational collapse can go either way, as shown in figure 4. Some of the axion clumps with initial conditions near the phase boundary emit enough axion radiation to avoid forming a black hole. This seems to happen erratically. A similar phenomenon was observed for the collapse of non-self interacting scalar fields in Ref. [21], where the effect was ascribed to gravitational cooling, using a term introduced for scalar field emission by collapsing boson stars in Ref. [6].

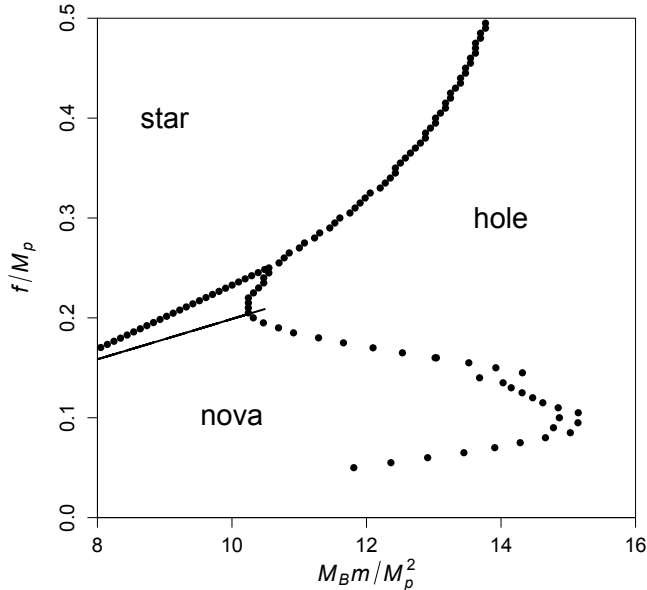


Figure 3. Phase diagram for axion scalar field collapse with axion mass  $m$ , scale parameter  $f$  and Bondi mass  $M_B$ , with  $M_p = (8\pi G)^{-1/2}$ . The thin line shows the maximum mass of a non-relativistic Bosenova with quartic self interaction. The boundary between black holes and Bosenovas is diffuse, and the plot shows only the largest mass initial condition which fails to form a black hole. The diagram is compiled using a bisection search technique, with retarded time range  $u = 10^3 m^{-1}$ . Trapped surface detection uses  $\bar{g}/g = 10^{-3}$  and the Bosenova is defined as a collapse of the core with central density  $\rho > 10^{-1} m^2 M_p^2$ . Some points have been checked using  $u = 2 \times 10^3 m^{-1}$  and  $\bar{g}/g = 10^{-4}$ .

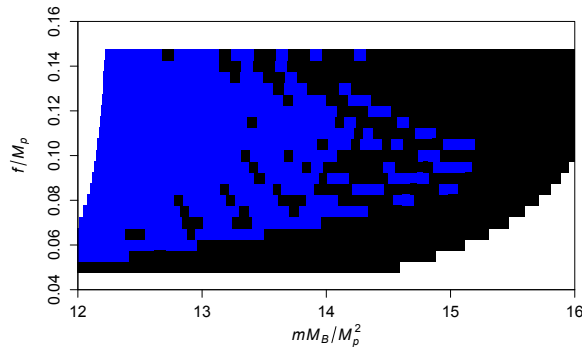


Figure 4. Part of the phase diagram where the phase boundary is diffuse. Each black pixel denotes a set of initial conditions which forms a black hole, and each blue pixel denotes a set of initial conditions which forms a Bosenova.

#### IV. DISCUSSION

Gravitational collapse with nothing more than gravity and a scalar field is a remarkably rich subject. It seems sensible to build up an understanding of it in small steps, the simplest being spherically symmetric collapse. We have considered three possible scenarios for axion collapse: axion stars, black holes and Bosenovas. The numerical results clearly point to a critical point with Bondi mass  $M_B \approx 10.6 M_p^2 m^{-1}$  and axion decay constant  $f \approx 0.25 M_p$  when the initial conditions are presented on a phase diagram. Mostly, the distinction between the different phases is clear, but in some parts of the phase diagram, there is no clean line between initial conditions which collapse to a black hole and those which remain non-singular. There may also exist special final states like the self-similar solutions for massless scalar collapse [12] which we have not considered.

The fate of a Bosenova is to eject mass until it eventually settles down into a stable axion star. In terms of the eventual outcome, the stars and Bosenova's are similar. However, the difference has a large physical significance for dark energy scenarios, since the axion radiation from many bursts and many sources would combine into a background of incoherent ALP particles.

Just how dependent the results are on the initial density profile and the use of null initial data surface may be determined through further work. The Gaussian initial density profile is known to work to within a few percent for results on non-relativistic Bose stars [23], but we have done some runs with radically different density profiles and find  $O(1)$  changes in the masses at the phase boundaries.

The null coordinate approach is fast, accurate and reliable, but it is limited to spherically symmetric collapse. It provides an important check on the results obtained from more sophisticated 3+1 integration schemes, but ultimately the 3+1 schemes are necessary for handling general collapse situations. We hope the clearer view of the simplest-case scenario considered here will help guiding future studies in this direction.

## ACKNOWLEDGMENTS

We would like to acknowledge useful discussions with Ruth Gregory and Gerasimos Rigopoulos. We are grateful for the hospitality of the Perimeter Institute, Waterloo, Canada where this paper was written. IGM and FM are supported by the Leverhulme grant RPG-2016-233. IGM also acknowledges some support from the Science and Facilities Council of the United Kingdom grant number ST/P000371/1.

- 
- [1] Pierre Sikivie, “Axion Cosmology,” *Axions: Theory, cosmology, and experimental searches. Proceedings, 1st Joint ILIAS-CERN-CAST axion training, Geneva, Switzerland, November 30-December 2, 2005*, *Lect. Notes Phys.* **741**, 19–50 (2008), [19(2006)], [arXiv:astro-ph/0610440 \[astro-ph\]](#).
  - [2] Asimina Arvanitaki, Savas Dimopoulos, Sergei Dubovsky, Nemanja Kaloper, and John March-Russell, “String Axiverse,” *Phys. Rev. D* **81**, 123530 (2010), [arXiv:0905.4720 \[hep-th\]](#).
  - [3] Hsi-Yu Schive, Tzihong Chiueh, and Tom Broadhurst, “Cosmic Structure as the Quantum Interference of a Coherent Dark Wave,” *Nature Phys.* **10**, 496–499 (2014), [arXiv:1406.6586 \[astro-ph.GA\]](#).
  - [4] C. J. Hogan and M. J. Rees, “Axion miniclusters,” *Phys. Lett.* **B205**, 228–230 (1988).
  - [5] Edward W. Kolb and Igor I. Tkachev, “Axion miniclusters and Bose stars,” *Phys. Rev. Lett.* **71**, 3051–3054 (1993), [arXiv:hep-ph/9303313 \[hep-ph\]](#).
  - [6] Edward Seidel and Wai-Mo Suen, “Formation of solitonic stars through gravitational cooling,” *Phys. Rev. Lett.* **72**, 2516–2519 (1994), [arXiv:gr-qc/9309015 \[gr-qc\]](#).
  - [7] D. G. Levkov, A. G. Panin, and I. I. Tkachev, “Relativistic axions from collapsing Bose stars,” *Phys. Rev. Lett.* **118**, 011301 (2017), [arXiv:1609.03611 \[astro-ph.CO\]](#).
  - [8] T. Helfer, D. J. E. Marsh, K. Clough, M. Fairbairn, E. A. Lim, and R. Becerril, “Black hole formation from axion stars,” *JCAP* **1703**, 055 (2017), [arXiv:1609.04724 \[astro-ph.CO\]](#).
  - [9] E.A. Donley, N.R. Claussen, S.L. Cornish, J.L. Roberts, E.A. Cornell, and C.E. Wieman, “Dynamics of collapsing and exploding Bose–Einstein condensates,” *Nature* **412**, 295 (2001), [arXiv:cond-mat/0105019](#).
  - [10] D. S. Goldwirth and T. Piran, “Gravitational collapse of massless scalar field and cosmic censorship,” *Phys. Rev. D* **36**, 3575–3581 (1987).
  - [11] D. Garfinkle, “Choptuik scaling in null coordinates,” *Phys. Rev. D* **51**, 5558–5561 (1995), [arXiv:gr-qc/9412008 \[gr-qc\]](#).
  - [12] Matthew W. Choptuik, “Universality and scaling in gravitational collapse of a massless scalar field,” *Phys. Rev. Lett.* **70**, 9–12 (1993).
  - [13] M. KusterGeorg, G. Raffelt, and B. Beltrán, *Axions* (Springer Berlin Heidelberg, 2008).
  - [14] J. E. Kim and G. Carosi, “Axions and the strong  $cp$  problem,” *Rev. Mod. Phys.* **82**, 557–601 (2010).
  - [15] A. Arvanitaki, S. Dimopoulos, S. Dubovsky, N. Kaloper, and J. March-Russell, “String axiverse,” *Phys. Rev. D* **81**, 123530 (2010).
  - [16] P. R. Brady, C. M. Chambers, and S. M. C. V. Goncalves, “Phases of massive scalar field collapse,” *Phys. Rev. D* **56**, R6057–R6061 (1997), [arXiv:gr-qc/9709014 \[gr-qc\]](#).
  - [17] C. Gundlach, R. H. Price, and J. Pullin, “Late-time behavior of stellar collapse and explosions. ii. nonlinear evolution,” *Phys. Rev. D* **49**, 890–899 (1994).
  - [18] R. Sachs, “Asymptotic symmetries in gravitational theory,” *Phys. Rev.* **128**, 2851–2864 (1962).
  - [19] J. D. Brown, S. R. Lau, and J. W. York, “Energy of isolated systems at retarded times as the null limit of quasilocal energy,” *Phys. Rev. D* **55**, 1977–1984 (1997).
  - [20] S. M. C. V. Goncalves and I. G. Moss, “Black hole formation from massive scalar fields,” *Class. Quant. Grav.* **14**, 2607–2615 (1997), [arXiv:gr-qc/9702059 \[gr-qc\]](#).

- [21] Miguel Alcubierre, Ricardo Becerril, Siddhartha F. Guzman, Tonatiuh Matos, Dario Nunez, and L. Arturo Urena-Lopez, “Numerical studies of  $\Phi^2$  oscillatons,” *Class. Quant. Grav.* **20**, 2883–2904 (2003), [arXiv:gr-qc/0301105 \[gr-qc\]](#).
- [22] Pierre-Henri Chavanis, “Instability of a uniformly collapsing cloud of classical and quantum self-gravitating Brownian particles,” *Phys. Rev.* **E84**, 031101 (2011), [arXiv:1103.5371 \[cond-mat.stat-mech\]](#).
- [23] Pierre-Henri Chavanis, “Collapse of a self-gravitating Bose-Einstein condensate with attractive self-interaction,” *Phys. Rev.* **D94**, 083007 (2016), [arXiv:1604.05904 \[astro-ph.CO\]](#).